Graph-Theoretical Analysis of Tunneling Electron Transfer in Large Polycyclic Aromatic Hydrocarbon Networks

Haruo Hosoya,* Sayaka Iwata, Minako Murokoshi, and Michiko Atsumi

Department of Information Sciences, Ochanomizu University, Bunkyo-ku, Tokyo 112-8610, Japan

Received June 30, 2000

Effect of a single nitrogen atom substitution to a number of large polycyclic aromatic hydrocarbon (PAH) molecules was calculated systematically, and it was found that especially in parallelogram-type PAH abnormal electron transfer (called tunneling electron transfer, TET) was observed. That is, fairly large amount of π-electron is withdrawn to an electronegative nitrogen atom from almost the farthest end of a conjugated aromatic hydrocarbon molecule, leaving almost no change in the interior of the molecule. This change can be simulated by the Kekulé structure counting for subgraphs of the parent molecule.

INTRODUCTION

The direction and extent of electron transfer in conjugated π-electron systems, though large, can now be understood and reproduced reasonably well by quantum chemical calculations. However, even before the introduction of quantum theory in chemistry, Robinson[1,2] and Ingold[3,4] were able to predict and "explain" the rough trend of electron transfer in conjugated hydrocarbons and their simple derivatives by the naive recipe of their organic electron theory with just a slight modification of the structural formula with curved arrows and induced charges $\delta+$ and $\delta-$.

This primitive theory has long prevailed[5−7] over all the organic chemists, supported by a huge amount of experimental facts in organic reactions. Most of the results are also supported by molecular orbital calculations, from Hückel[8] to ab initio methods for individual cases. However, there has never been given any mathematical proof for the general validity of this diagrammatic method. Very recently one of the present authors[9] succeeded in proving that the global trend of the direction and extent of the π-electron transfer in acyclic conjugated hydrocarbon molecules predicted by this recipe is correct by the combined use of the graph-theoretical technique and atom-atom polarizability proposed by Coulson and Longuet-Higgins.[10] For cyclic conjugated systems with a few benzene rings this recipe was shown to be applied similarly to the case of acyclic π-electron systems.

However, it is to be noted here that the rate of damping of electron transfer along the long π-electronic system cannot be predicted by formal application of the diagrammatic method.[11] During the course of analysis along this line one of the well-accepted reactivity indices, superdelocalizability (S_r), of Fukui et al.[12] for infinitely large polyene, polyacetylene, was found to diverge.[13] This finding is in marked contrast to their assertion that the relative magnitudes of the various reactivity indices, atom-atom polarizability ($\pi_{r,r}$), free valency (F_r), localization energy (L_r), frontier electron density (f_r), and S_r, within a molecule are in parallel with each other. It is thus suggested that even in the established kingdom of Hückel molecular orbital theory (HMO) there still remain unexplored mines, especially in the domain of large polycyclic aromatic hydrocarbons (PAHs). Actually during our study by the combined use of HMO, Kekulé structure counting, and graph theory, we could find an excitingly new phenomenon, namely, tunneling electron transfer, in large PAH networks.

ELECTRON TRANSFER IN LINEAR POLYACENES

Let us denote a parallelogram-type PAH composed of m-layered polyacenes as P(m,n) (See Figure 1a). The so-called polyacene is denoted by P(1,n). Naive application of the diagrammatic recipe of organic electron theory yields Figure 2, which, however, is unrealistic, because no damping of electron transfer is taken into account. Let us then study this problem.

First consider anthracene, P(1,3), and compare the mode of electron withdrawal from the peripheral carbon atoms by substituting an electronegative nitrogen atom at α- and β-positions. The $\delta\pm$ values on the peripheral carbon atoms of α- and β-substituted anthracenes can directly be calculated by putting the Coulomb parameter for the substituted atom as $\alpha + \beta$. According to Coulson and Longuet-Higgins[10] the charge density change δq_s at atom s is calculated to be the product of the atom-atom polarizability $\pi_{r,s}$ and the increment $\delta\alpha_r$ at the substituted atom r of the parent hydrocarbon. By putting $\delta\alpha_r = \beta$, δq_s becomes equal to $\pi_{r,s}$. For small PAHs this perturbation approximation reproduces rather accurately the $\delta\pm$ values obtained from the direct calculation as shown in Figure 3 for α-and β-substituted anthracenes. If the point of heteroatom substitution belongs to the starred-atom group, $\delta+$ appears only at the unstarred carbon atoms, while $\delta-$ at the starred. This property can be explained straightforwardly by the pairing theorem established by Coulson and Rushbrooke.[15]

Similar calculations were performed for higher members of linear polyacenes, P(1,n). The pattern of the $\delta\pm$ values rapidly converges to what is essentially the same for the substituted anthracenes. This means that in polyacene, though large, the π-electron is confined to transfer rather locally as shown in Figure 3.

10.1021/ci0000732 CCC: $20.00
Published on Web 05/02/2001

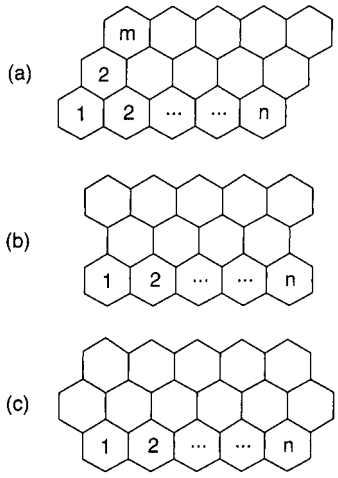

Figure 1. Three different types of PAH networks studied in this paper. (a) Parallelogram-type, P(*m*,*n*), (b) X-type, X(*n*), and (c) O-type, O(*n*).

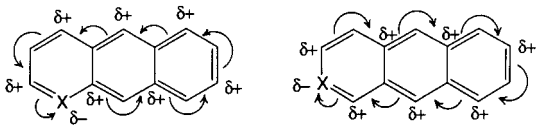

Figure 2. Diagrammatic π-electron flow in substituted anthracene as expected from organic electron theory if damping is not taken into account.

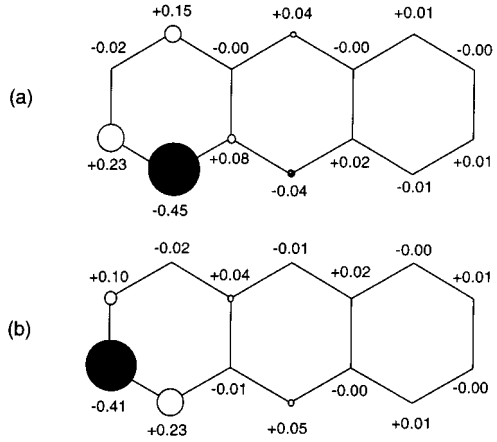

Figure 3. The $\delta\pm$ values of the peripheral carbon atoms of (a) α-isomers and (b) β-isomers of nitrogen-substituted anthracenes estimated from $\pi_{r,s}$ of anthracene.

However, it is important to scrutinize both patterns in Figure 3 more carefully. The following features were detected.

(1) Degree of π-electron withdrawal from the ortho atoms is almost the same for α- and β-substitutions.

(2) The α-substituted heteroatom withdraws more π-electron from the para position than β-substitution.

(3) A very small amount of negative charge is induced at the meta positions for both substitutions.

(4) Damping rate of the $\delta+$ value is roughly proportional to the reciprocal of the distance from the substituted atom, while $\delta-$ exponentially decreases.

Note that features 3 and 4 were also observed for polyacetylene. Further, it became clear that the diagrammatic recipe used in organic electron theory can predict only feature 1 for PAHs.

TUNNELING ELECTRON TRANSFER IN PARALLELOGRAM NETWORKS

Calculations were then extended to a large number of P(*m*,*n*) networks together with the series of perylene (X(*n*)) and coronene (O(*n*)) type PAHs (see Figure 1). Since it was found that for infinitely large P(*m*,*n*) networks $\pi_{r,s}$ tends to diverge, [13] hereafter only the results of direct calculations will be given. For these series of pericondensed aromatic hydrocarbons, abnormal electron transfer across large π-electron networks was observed, especially markedly for P(*m*,*n*)'s with $m > 2$.

Striking examples are shown in Figure 4, where charge densities of extremely large α-substituted P(*m*,39) with $m = 2$, 3, and 8 are given. By a substitution of a single nitrogen atom at one of the terminal carbons (marked with a big arrow) of the P(8,39) network, the interior π-electrons are unaffected and only those on the peripheral carbon atoms are perturbed. A big tide of electron wave comes from the opposite but not the farthest end of the network. The largest seismic intensity is observed at the peripheral carbon in the 35th benzene ring out of 39 counting from the left end of the shore opposite the epicenter. Along the same shore of the epicenter a fairly large amount of excess π-electron is accumulated, which not only classical organic theory but also modern common understanding of π-electron behavior can hardly anticipate. The π-electronic dipole moment of this hypothetical molecule was calculated to be as large as 300 D, suggesting potential applicability of these substances to useful electronic devices. Let us call this abnormal phenomenon tunneling electron transfer (TET). From Figure 4 one can observe that the length of tunneling in the P(*m*,*n*) network increases with the thickness (*m*) of the parallelogram. A more precise observation was applied to the series of P(*m*,*n*) with $m = 1-6$. Namely, Figure 5 shows the limiting values of the "normalized" peak positions of $\delta+$ for various series of parallelogram-type PAHs caused by nitrogen substitution at the α-carbon atom. Then the peak $\delta+$ value in the opposite edge was found to occur roughly at the normalized distance of $(m - 1)/m$ (for $m > 2$) from the left corner. This is a challenging problem to be explained.

Further, it is interesting to observe that TET does not occur for heteroatom substitution at the β-position. Figure 6 shows that when a nitrogen atom is substituted in P(3,7) global TET is observed for the substitution at the α-position and the positions belonging to the same (starred or unstarred) group, while only local change is observed for β-group substitution. In each case the largest filled circle indicates the magnitude of $\delta-$ caused by nitrogen substitution at that carbon atom. Such a large difference in the mode of π-electron transfer cannot be differentiated by the classical organic electron theory.

If the values of $\pi_{r,s}$ for all the pairs of atoms are available[16,17] for a given PAH network, one can predict relative magnitudes of π-electron transfer between atoms r and s. Although until recently there has never been known any effective and simple index for estimating the magnitude of $\pi_{r,s}$, we could obtain the rules for judging the relative magnitude of $\pi_{r,s}$ for a pair of atoms, r and s, of an acyclic conjugated systems.[9] Since all the acyclic hydrocarbons are

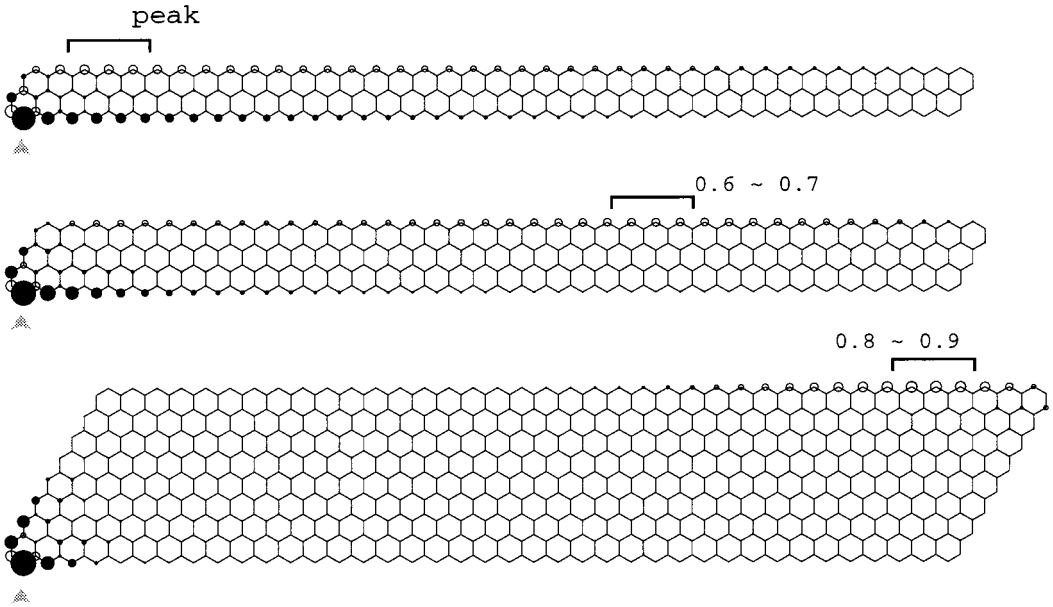

Figure 4. Tunneling electron transfer in parallelogram-type PAH. The largest arrow indicates the position of nitrogen atom substitution. Filled circles, $\delta-$; open circles, $\delta+$. Small arrow indicates the position of peak $\delta+$.

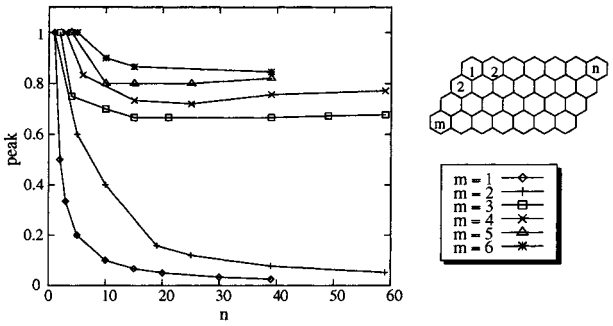

Figure 5. The limiting value of "normalized" distance to the site of the largest $\delta+$ measured from the left end of the opposite edge for various P(m,n) series with $m = 1-6$.

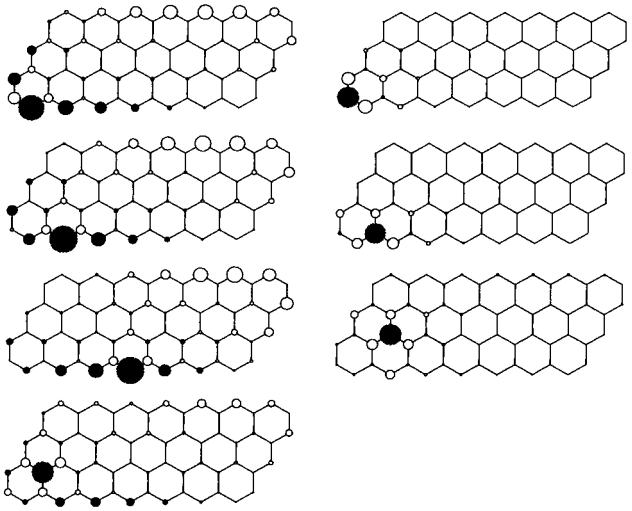

Figure 6. (a) Global TET and (b) local electron transfer observed, respectively, in α- and β-substitution with a nitrogen atom to P(3,7). The largest filled circle indicates the position of nitrogen atom substitution. Filled and open circles, respectively, represent $\delta-$ and $\delta+$.

alternant, the component carbon atoms can be grouped into starred and unstarred.[10,15] Then the rules can be stated as follows:

(1) For (r,s) pair of the same group $\pi_{r,s}$ is positive (giving $\delta-$ for nitrogen substitution), and rapidly decreases (almost exponentially) with the distance between r and s.

(2) For (r,s) pair of different groups $\pi_{r,s}$ is negative (giving $\delta+$ for nitrogen substitution), and $|\pi_{r,s}|$ slowly decreases with the distance between r and s, or roughly proportional to $Z_{G\ominus\overline{rs}}$.

(3) For cross-conjugation, even for (r,s) pair of different groups, $\pi_{r,s}$ becomes zero if $K(G\ominus\overline{rs})$ is zero.

Let us add a supplementary explanation for rules 2 and 3. $G\ominus\overline{rs}$ is the subgraph of graph G obtained by deleting the path $\overline{rs}$ together with all the attached edges (C−C bonds).[18] Z is the topological index, which was proposed by one of the present authors.[18] K(G) denotes the number of Kekulé structures for G. With these features for acyclic polyenes in mind, let us observe carefully the distribution of $\delta\pm$ in Figure 6.

It is to be noted that in the left half of Figure 6, where global TET is observed, the peripheral atoms situating on the left and lower edges are starred and negatively charged, while the atoms on the right and upper edges are unstarred and positively charged. Rule 1 seems to be applied similarly to PAHs. Rules 2 and 3 are dependent on the path between r and s, which is composed of successively conjugated C=C double bonds. Although for acyclic systems the path $\overline{rs}$ is uniquely determined, for cyclic conjugated systems, especially for PAHs, there exist a large number of paths between a given pair of atoms, each of which is contributing to the total π-electron transfer between them.

For example, even for a smaller member, such as P(2,3), nearly 20 different paths are possible for a special pair of atoms besides as many unacceptable paths with zero $K(G\ominus\overline{rs})$ as shown in Figure 7. The quantity $\pi_{r,s}$ is decomposed into the contributions from all the possible paths with the weight of $K(G\ominus\overline{rs})$. Thus this decomposition is a rather tedious task for PAHs.

Thus instead of taking all the possible paths connecting r and s, we have chosen such a bold assumption that subgraph

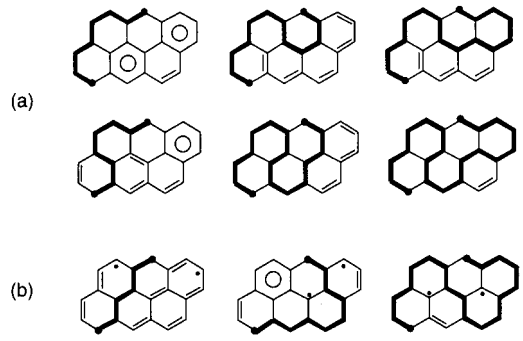

Figure 7. Examples of (a) acceptable and (b) unacceptable paths for a special atom pair of P(2,3).

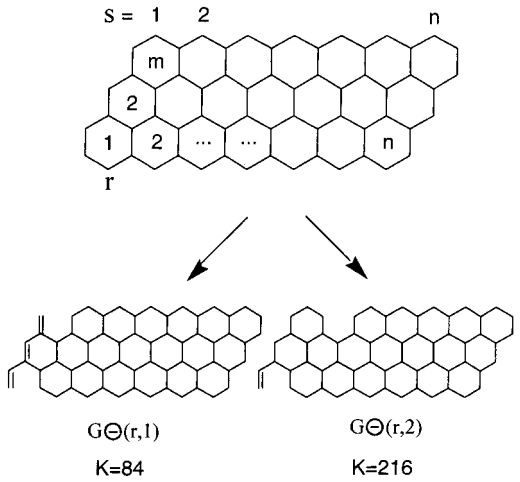

Figure 8. Examples of subgraph GΘ(r,s) of P(*m*,*n*). The number of Kekulé structures of P(*m*,*n*)Θ(r,s) are given in Table 1.

GΘ(r,s), obtained from G by deleting vertices r and s, represents the sum of all the possible contributions arising from the (r, s) pair. This assumption can be paraphrased in terms of the mathematical expressions for the topological polarizability. Namely, we take

$$\pi^{T}_{r,s} = K(G\Theta(r,s)) \quad (1)$$

instead of

$$\pi^{T}_{r,s} = \sum_{k} \{K(G\Theta\overline{rs}_k)\, Z_{G\Theta\overline{rs}_k}\} \quad (2)$$

where $\overline{rs}_k$ means the *k*th path connecting atoms r and s.

KEKULÉ STRUCTURE COUNT

Then try to calculate the numbers of Kekulé structures for a special case. Choose again the network P(3,7) as treated in Figure 6. The number of Kekulé structures, *K*(G), for parallelogram-type PAH, P(*m*,*n*), is known to be

$$\binom{m+n}{m} = (m+n)!/\{m!n!\} \quad \text{(refs 19−21)}$$

The site of nitrogen substitution, atom r, is taken at the α-carbon atom in the benzene ring located at the lower left hand corner, and atom s is chosen from the upper edge of the network. Then as in Figure 8 *K*(G)'s for the series of subgraphs, P(3,7)Θ(r,s), are calculated for $s = 1-7$. Note that for a special case $K(P(m,n)\Theta(r,1)) = K(P(m,n-1))$.

Table 1. Values of *K*(GΘ(r,s)), δq_s, and $\pi_{r,s}$ for Network P(3,7)[a]

s	K(GΘ(r,s))	δq_s	$\lvert\pi_{r,s}\rvert$
1	84	0.010	0.022
2	216	0.048	0.102
3	360	0.104	0.217
4	480	0.157	0.319
5	540	0.181	0.354
6	504	0.149	0.282
7	336	0.064	0.118

[a] See the caption of Figure 9 for explanation of the molecular diagram.

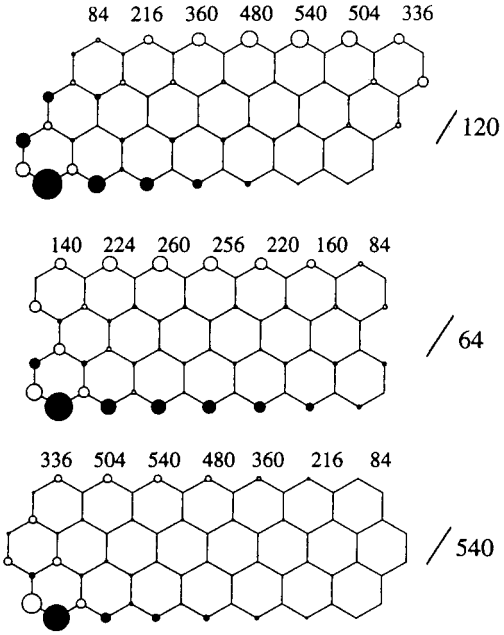

Figure 9. Comparison of the δ± distribution by nitrogen substitution and *K*(G) values for the corresponding subgraphs calculated for PAHs of P(*m*,*n*) and X- and O-types. The radius of a circle is proportional to δ±, while the numeral gives the *K*(G) value for the subgraph obtained by deleting that atom and the atom marked with the largest filled circle. The number following the slash is the *K*(G) of the parent molecule.

Further, a general expression for *K*(G) of these subgraphs was obtained as

$$K(P(m,n)\Theta(r,s)) = s(s+1)(s+2)...(s+m-2)(n+1)(n+2)...(n+m-1)(n-s+1)/\{m!(m-1)!\} \quad (s = 1, ..., n) \quad (3)$$

General proof is rather tedious, but the results are correct as given in Table 1, where $m = 3$ and $n = 7$. In Figure 9a those *K*(GΘ((r,s) values are compared with the δ± values for nitrogen substitution. Correlation between the *K*(G) and δ± values (together with $\pi_{r,s}$) is amazingly good.

Note that the *K*(G)'s for all the subgraphs, P(*m*,*n*)Θ(r,s), except for $s = 1$ are larger than that of the parent parallelogram. This means that a π-electron network of PAH with parallelogram shape is intrinsically so unstable that it is stabilized by degradation of conjugated network. A similar phenomenon has been known in organic chemistry. That is, long unstable polyacene is easily stabilized to form quinone by degrading the conjugated network. In this case also the *K*(G) of the parent molecule is smaller than the product of the *K*(G)'s of smaller fragments.[22]

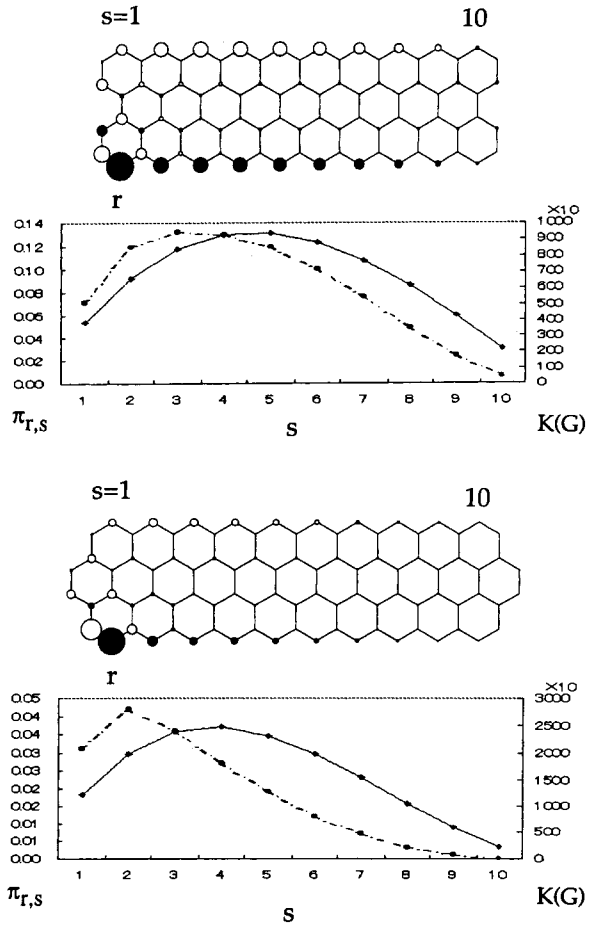

Figure 10. Relation between the polarizability $\pi_{r,s}$ and K(G) for X- and O-type PAHs. See also the caption of Figure 9.

One can differentiate eq 3 with respect to s, and obtain the value of s for yielding maximum K(G). Instead of pursuing straightforward analysis, differentiation for the individual cases with smaller values of m, say up to 5, was executed. After surveying the set of the obtained results, one can induce the following clear result, $s_{max} = (m - 1)/m$, which is exactly the same as our former observation. Now we believe that this is the secret of the abnormal TET observed in heteroatom substitution to parallelogram-shaped PAHs.

OTHER SERIES OF PAHS

We have performed similar calculations for two other series of PAHs, perylene-type X(n)'s and coronene-type O(n)'s (Figure 1). The results are given in Figure 9b,c and Figure 10. X-type molecule is always stabilized by degradation, while O-type molecule is destabilized. In both types the magnitude of TET is rather smaller than the case of P-type. It is generally known that O-type is the most stable among the three types of P, O, and X, while X-type the least stable.[23] As seen in Figure 9b, the TET pattern of X-type is rather symmetrical to the line dissecting the central polyacene moiety. Thus we can say that the most interesting TET is observed in P(m,n).

As shown in Figure 10, correlation between the $\delta\pm$ distribution and K(G) values is not as good for X- and O-type PAHs. However, with the increase of the size and thickness of these types the correlation gets rather better. Then the bold assumption which we have made above must have deep physical meaning. Let us restate that assumption. That is, a single subgraph G$\ominus$(r,s) (see eq 1), obtained from a large PAH network, G, by deleting vertices r and s, represents the total sum of all the possible contributions (see eq 2) arising from the pair of atoms (r, s). This is an open question.[24]

REFERENCES AND NOTES

(1) Robinson, R. Polarization of Nitrosobenzene. *J. Soc. Chem. Ind.* **1925**, *44*, 456−458.
(2) Robinson, R. *Outline of an Electrochemical Theory of the Course of Organic Reactions*; Inst. Chem. Great Britain and Ireland: London, 1932.
(3) Ingold, C. K. Principles of an Electron Theory of Organic Reactions. *Chem. Rev.* **1934**, *15*, 225−274.
(4) Ingold, C. K. *Structure and Mechanism in Organic Chemistry*; Cornell University Press: Ithaca, 1953.
(5) Pauling, L. *The Nature of the Chemical Bond*; Cornell University Press: Ithaca, 1960.
(6) Wheland, G. W. *The Theory and Resonance and Its Application to Organic Chemistry*; Wiley: New York, 1944.
(7) Branch, G. E. K.; Calvin, M. *The Theory of Organic Chemistry*; Prentice-Hall: New York, 1945.
(8) Streitwieser, A. *Molecular Orbital Theory for Organic Chemists*; Wiley: New York, 1961.
(9) Hosoya, H. Mathematical Foundation of the Organic Electron Theory—How Do π-Electrons Flow in Conjugated Systems? *J. Mol. Struct.* (*THEOCHEM*) **1999**, *461*−*462*, 473−482.
(10) Coulson, C. A.; Longuet-Higgins, H. C. The Electronic Structure of Conjugated Systems. I. *Proc. R. Soc*., *A* **1947**, *191*, 39−60.
(11) Although it is implicitly accepted in organic electron theory[1−4] that mesomery effect decreases with the distance from the point of heteroatom substitution, no quantitative description has been given.
(12) Fukui, K.; Yonezawa, T.; Nagata, C. Interrelations of Quantum-Mechanical Quantities Concerning Chemical Reactivity of Conjugated Molecules. *J. Chem. Phys.* **1957**, *26*, 831−841.
(13) Hosoya, H. Revisiting Superdelocalizability. Mathematical Stability of Reactive Indices. *Theor. Chem. Acc.* **1999**, *102*, 293−299. See also ref 14 on the divergence of S_r.
(14) Ishihara, M. Superdelocalizability of Linear Chains. *Bull. Chem. Soc. Jpn*. **1997**, *70*, 1307−1310.
(15) Coulson, C. A.; Rushbrooke, G. S. The Method of Molecular Orbitals. *Proc. Cambridge Philos. Soc.* **1940**, *36*, 193−200.
(16) Streitwieser, A. Jr.; Brauman, J. I. *Supplemental Tables of Molecular Orbital Calculations*; Pergamon Press: Oxford, 1965.
(17) Coulson, C. A.; Streitwieser, A. Jr. *Dictionary of π-Electron Calculations*; Pergamon Press: Oxford, 1965.
(18) Hosoya, H. Topological Index. A Newly Proposed Quantity Characterizing the Topological Nature of Structural Isomers of Saturated Hydrocarbons. *Bull. Chem. Soc. Jpn*. **1971**, *44*, 2332−2339.
(19) Yen, T. F. Resonance Topology of Polynuclear Aromatic Hydrocarbons. *Theor. Chim. Acta* **1971**, *20*, 399−404.
(20) Hosoya, H. Matching and Symmetry of Graphs. *Comput. Math. Appl*. **1986**, *12B*, 271−290.
(21) Cyvin, S. J.; Gutman, I. *Kekulé Structures in Benzenoid Hydrocarbons*; Lecture Notes in Chemistry 46; Springer: Berlin, 1988.
(22) Ohkami, N.; Hosoya, H. Topological Dependency of the Aromatic Sextets in Polycyclic Hydrocarbons. Recursive Relations of the Sextet Polynomial. *Theor. Chim. Acta* **1983**, *64*, 153−170.
(23) Dias, J. R. Isomer Enumeration and Topological Characteristics of Benzenoid Quinones. *J. Chem. Inf. Comput. Sci*. **1990**, *30*, 53−61.
(24) Our preliminary calculation shows that the values of $Z_{G\ominus(r,s)}$ remain almost constant during the scanning of atom s along the edge of a given PAH and with r atom being fixed.

CI0000732